Research Article

Raghad R. Alzahrani*, Manal M. Alkhulaifi*, and Nouf M. Al-Enazi

In vitro biological activity of *Hydroclathrus clathratus* and its use as an extracellular bioreductant for silver nanoparticle formation

https://doi.org/10.1515/gps-2020-0043
received April 22, 2020; accepted June 28, 2020

Abstract: The adaptive nature of algae results in producing unique chemical components that are gaining attention due to their efficiency in many fields and abundance. In this study, we screened the phytochemicals from the brown alga *Hydroclathrus clathratus* and tested its ability to produce silver nanoparticles (AgNPs) extracellularly for the first time. Lastly, we investigated its biological activity against a variety of bacteria. The biosynthesized nanoparticles were characterized by UV-visible spectroscopy, Fourier-transform infrared spectroscopy, dynamic light scattering, transmission electron microscopy, and energy-dispersive spectroscopy. The biological efficacy of AgNPs was tested against eighteen different bacteria, including seven multidrug-resistant bacteria. Phytochemical screening of the alga revealed the presence of saturated and unsaturated fatty acids, sugars, carboxylic acid derivatives, triterpenoids, steroids, and other components. Formed AgNPs were stable and ranged in size between 7 and 83 nm and presented a variety of shapes. *Acinetobacter baumannii*, *Staphylococcus aureus*, Methicillin-resistant *S. aureus* (MRSA), and MDR *A. baumannii* were the most affected among the bacteria. The biofilm formation and development assay presented a noteworthy activity against MRSA, with an inhibition percentage of 99%. Acknowledging the future of nano-antibiotics encourages scientists to explore and enhance their potency, notably if they were obtained using green, rapid, and efficient methods.

Keywords: brown algae, silver nanoparticles, biosynthesis, bio-nanoparticles, MDR bacteria

Abbreviations

AgNPs	silver nanoparticles
$AgNP_{CB}$	silver nanoparticles synthesized by *H. clathratus* crude methanol extract
$AgNP_{QB}$	silver nanoparticles synthesized by *H. clathratus* aqueous solution
ATCC	American Type Culture Collection
DLS	dynamic light scattering
DMSO	dimethyl sulfoxide
EDS	energy-dispersive spectroscopy
FTIR	Fourier-transform infrared spectroscopy
TEM	transmission electron microscopy

1 Introduction

Despite the progress of bacterial resistance to antibiotics, the development of a new, effective antibiotic against multidrug-resistant (MDR) bacteria has been progressing at a slow pace. Recent studies have suggested using nanotechnology as a promising strategy to challenge bacterial resistance to antibiotics using natural constituents as reducing agents to synthesize nanoparticles (NPs), although this approach could be limited due to the toxicity and unpredictability of NPs [1]. There were several cases that reported the existence of MDR bacteria in Saudi Arabia. For example, a few cases of MDR tuberculosis in different regions of Saudi Arabia were observed [2]. Besides, prevalence rates of extended-spectrum beta-lactamase (ESBL) producing isolates, such as *Escherichia coli* and *Klebsiella pneumoniae*, were 29% and 65%, respectively [3]. Bacterial biofilm formation is a significant virulence factor that aids in antibiotic resistance and bacterial survival, especially on

* **Corresponding author: Raghad R. Alzahrani,** Department of Botany and Microbiology, College of Science, King Saud University, Riyadh 11451, Saudi Arabia, e-mail: raghad.r.alzahrani@gmail.com
* **Corresponding author: Manal M. Alkhulaifi,** Department of Botany and Microbiology, College of Science, King Saud University, Riyadh 11451, Saudi Arabia, e-mail: manalk@ksu.edu.sa
Nouf M. Al-Enazi: Department of Biology, College of Science and Humanities in Al-Kharj, Prince Sattam Bin Abdulaziz University, Al-Kharj 11942, Saudi Arabia, e-mail: n.alenazi@psau.edu.sa

medical devices [4]. Seaweeds are considered as promising sources of new antibacterial agents. More than one thousand bioactive components from a marine source, including algal secondary metabolites, have been globally defined as possible antibacterial, antiviral, anti-inflammatory, and anticancer agents [5]. Brown algae are known in the field of medicine and nutrition. Their medical history goes back to time when they were used for treating diarrhea, urinary disorders, and chronic bacterial infections in Europe [6]. Their cell walls comprise a distinct variety of bioactive polysaccharides, as well as fewer amounts of phenolic substances, proteins, and halide compounds such as iodide [7]. The thallus of *Hydroclathrus clathratus* appears perforated in a sponge resembling form; hence, its Latin name *clathratus* means *latticed*, indicating its morphology. The alga is distributed worldwide in warm seas and calm, shallow areas such as Europe, both coasts of Africa, the Pacific Islands, Asia, Australia, North America, and South America, from California through Chile and the Gulf of Mexico [8]. Algal phytochemicals contain functional groups, such as hydroxyl, carboxyl, and amino groups, which are beneficial for the reduction and capping process required to synthesize a stable and robust coating on metal NPs [9]. Scientists recommend algae in biological NP synthesis, due to their high metal uptake capacity and their minimal cost of production, which are golden advantages, compared to other bioreductants [10]. This study aims to screen the phytochemicals of the brown alga *Hydroclathrus clathratus* (methanol extract and raw powder). Then, we investigate its bioreducing ability of silver nitrate to silver nanoparticles (AgNPs) and explore its biological activity as an antibacterial and antibiofilm agent against a number of pathogenic bacteria, including MDR bacteria.

2 Materials and methods

2.1 Algae collection and preparation

H. clathratus (Figure 1) was collected from the northwest coast of Al-Haraa, Umluj City, Red Seashore, Kingdom of Saudi Arabia, in April 2017. The algae were kept in ice packs in plastic bags containing seawater for preservation. They were then washed and shade dried at room temperature and finely powdered using an electric coffee grinder. The algae were then preserved in tight dark containers in the freezer before use. *H. clathratus* was identified, according to [11,12].

2.2 Crude methanol extraction

H. clathratus (219 g) was saturated three times in 1 L of methanol for 72 h. The mixture was agitated (WNB shaker) to ensure constant agitation during the saturation procedure. Methanol extracts were collected,

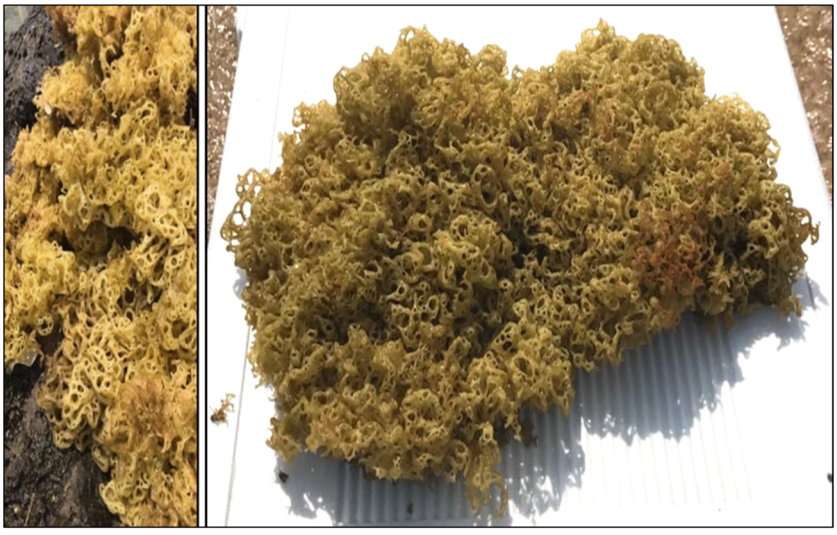

Figure 1: *Hydroclathrus clathratus* on the collection site.

filtered, and combined. The combined extract was concentrated by evaporating methanol on a rotavapor at ±50°C; after evaporating the solvent, the sample was preserved at room temperature. At the onset of each biological test, a stock solution was prepared at a concentration of 100 mg/mL in 100% DMSO. The extract was then kept in a sterile tube at 4°C until use.

2.3 Raw algal powder solution preparation

To prepare the raw algal powder, 5 g of the powdered algae was added to 100 mL of distilled water for easier handling. The mixture was agitated on a magnetic stirrer for 5 h at room temperature and then filtered. The filtrate was then kept in a sterile dark lid flask at 4°C.

2.4 Qualitative phytochemical screening of algal powder and methanol extract

We studied the chemical compositions of both the algal crude methanol extract and the raw powder by gas-chromatography mass spectroscopy (GC-MS) on the Shimadzu model 2010 plus (Japan). The samples were prepared as follows: 247 mg of raw algal powder was dissolved in 20 mL of 3:1 dichloromethane to methanol; in contrast, 104 mg of algal methanol extract was dissolved in 20 mL of methanol. The samples were then analyzed by GC-MS, according to the following parameters. The MS model QP 2010 ultra and injector model AOC-20i were used and operated in total ion chromatogram scan mode and single ion monitoring ion mode to obtain the retention time of each unidentified compound in the mixture extract samples. After adjustment, we obtained sufficient and adequate separation.

2.5 Biological synthesis of AgNPs

The biological synthesis of AgNPs was conducted after modifying the procedure used by [13]. Algal methanol extract stock (3 mL) and the aqueous solution (3 mL) were added dropwise into a flask containing 22 mL of 1 mM $AgNO_3$ aqueous solution. The flasks were then exposed to heat (50°C) to reduce the reaction time. Color change to brown was the visual assessment of AgNPs' formation for the algal aqueous solution ($AgNP_{QB}$); however, due to intensity of the green chlorophyll pigment in the NPs formed by the methanol extract ($AgNP_{CB}$), it was essential to use UV-vis spectroscopy to confirm their formation.

2.6 Characterization of biosynthesized silver NPs

The obtained AgNPs were first characterized by UV-vis spectroscopy (Libra S60PC) in the range between 350 and 750 nm. The morphological assessment of AgNPs was conducted using both transmission electron microscopy (TEM) [JEM 1400] at 80 kV accelerating voltage and dynamic light scattering (DLS) (Nano ZS zetasizer system [Malvern Instruments]), which was also used to clarify the dispersity of formed NPs. Fourier-transform infrared spectroscopy (FTIR) [PerkinElmer FTIR system spectrum BX] was used to investigate the involvement of functional groups in the formation of AgNPs in the range between 4,000 and 400 cm^{-1}. Lastly, evaluation of the elemental silver percentage was performed by energy-dispersive spectroscopy (EDS) [JSM-6380 LA].

2.7 Antibacterial activity of biologically synthesized AgNPs

Agar well-diffusion assay and minimum bactericidal concentration (MBC) on agar were performed following The National Committee for Clinical Laboratory (2006) standards. The minimum inhibitory concentration (MIC) assay was performed following [14], with a few modifications. The tested concentration range varied from 18 to 0.035 mg/mL. All experiments were repeated three times and evaluated in comparison to the positive and negative controls.

2.8 Tested bacteria and media

The biologically obtained AgNPs were tested against eighteen bacteria, including seven MDR bacteria. Pure cultures of bacterial strains were obtained from the Microbiology laboratory, in Prince Sultan Military Medical City, Riyadh. The bacteria were first cultured on sheep blood agar (Oxoid) before each experiment. Mueller–Hinton agar was used in the agar well-diffusion

assay, and 80 µL of tested AgNPs was loaded into 6 mm wells in the agar. Mueller–Hinton Broth was used in the MIC assay and SBA was used in the MBC assay. All tested plates were incubated at 37°C for 18–24 h.

2.9 Biofilm growth and development inhibition assay of biologically synthesized AgNPs

$AgNP_{CB}$ were tested for their antibiofilm ability in triplicate. Six biofilm-forming bacteria were tested (MDR *A. baumannii*, MDR *P. aeruginosa*, MRSA, *A. baumannii*, *P. aeruginosa*, and *S. aureus*). The protocol was adapted from [15] with modifications. The assay was performed in a 96-well flat-bottom microplate. The brain–heart infusion broth medium was used. For the biofilm quantitative analysis, we used crystal violet (CV) stain 1% (w/v) aqueous solution. Next, the microplates were destained and examined optically using an ELISA reader (EMax® Endpoint ELISA Microplate Reader) at OD_{450} nm. The results were averaged, prior to calculating the inhibition percentage using the formula [16]:

$$\text{Percentage of inhibition (\%)} = [1 - (A_{\text{Treated Well 450 nm}} - A_{\text{Untreated control 450 nm}}) \times 100] \quad (1)$$

2.10 Statistical analysis

Each test was tested three times for repetitions; means and standard deviations were obtained using Microsoft Excel 16.19.

3 Results

3.1 Qualitative phytochemical screening of algal powder and methanol extract

We were able to separate more than 60 components. The isolated phytochemicals included saturated and unsaturated fatty acids, sugars, carboxylic acid derivatives, triterpenoids, steroids, and other components such as alkenes and phytols (Table 1).

Table 1: Major components present in *H. clathratus* methanol extract and powder, and their percent relative concentration

Component	Percent relative concentration (%)	
	H. clathratus MeOH	*H. clathratus* powder
Hexadecanoic acid	21.67	21.51
Oleic acid	13.18	15.32
Octadecanoic acid	2.59	23.65
Tetradecanoic acid	8.68	7.08
Glyceryl-glycoside	2.13	0
Others	51.75	32.44

3.2 Characterization of biosynthesized AgNPs

3.2.1 UV-visible spectroscopy (UV-vis)

The confirmation of AgNPs' formation was assessed visually by a color change. However, due to the intensity of the green pigment in the algal methanol extract, a spectroscopic analysis was required. Biosynthesis of $AgNP_{CB}$ occurred shortly after adding the algal extract (within 1 h), and the highest absorption peak was evident at 411 nm (Figure 2a). In contrast, $AgNP_{QB}$ biosynthesis was monitored for a month; due to the slow formation of AgNPs, the formation of $AgNP_{QB}$ manifested at day 11 and was increased consistently. The highest peak was recorded on the 29th day at 451 nm (Figure 3a). Next, the sample was set for other characteristic techniques and biological tests.

3.2.2 DLS

Zeta size was used to investigate the particle size and distribution of AgNPs. Furthermore, it was used to determine the stability of obtained AgNPs in reference to the polydispersity index (PDI) value. $AgNP_{CB}$ showed an average NP size of 136.9 d.nm and PDI of 0.139 (Figure 2b), implicating the high stability and narrow size distribution of AgNPs. $AgNP_{QB}$ presented an average particle size of 83 d nm and PDI of 0.196 (Figure 3b), signifying its narrow size distribution and high stability.

3.2.3 TEM

TEM was used to study the morphological features such as shape and size of biosynthesized AgNPs. The

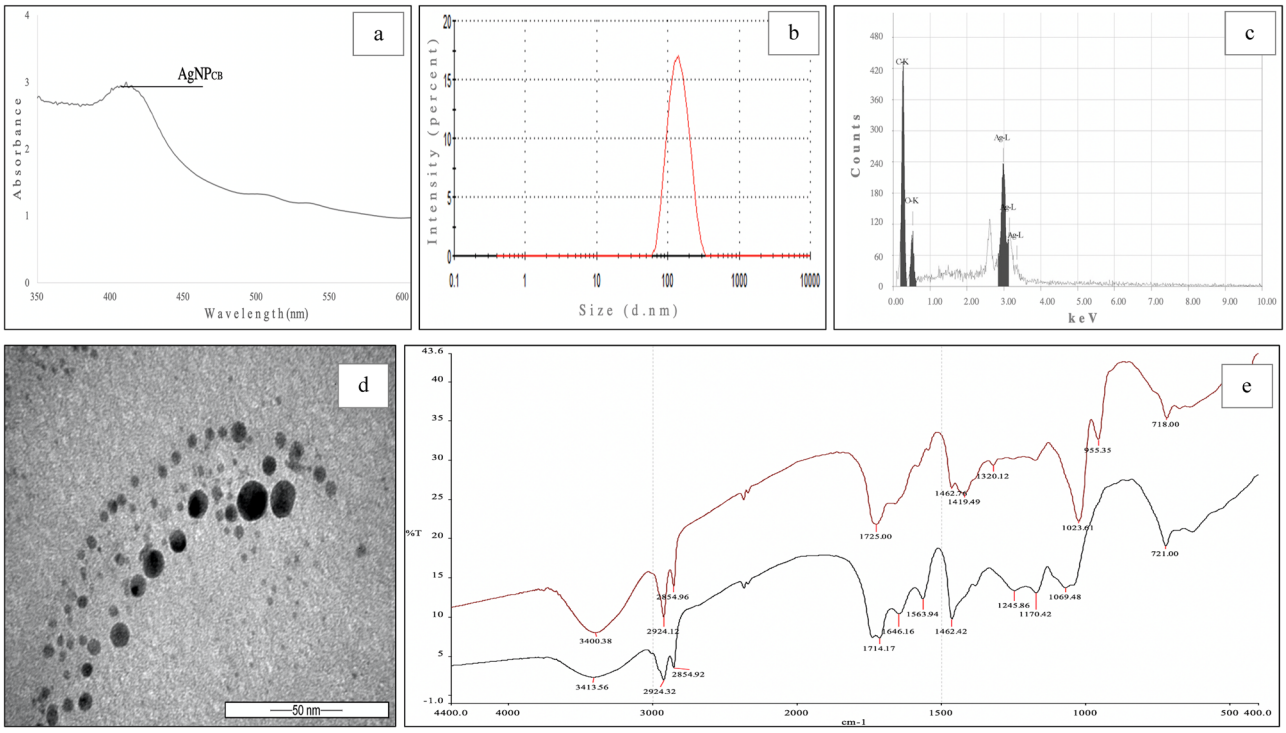

Figure 2: Characterization of biosynthesized $AgNP_{CB}$ by: (a) UV-vis spectroscopy, (b) DLS, (c) EDS of $AgNP_{CB}$ presenting 30% of Ag, (d) TEM imaging, and (e) FTIR of *H. clathratus* crude methanol extract before (black) and after $AgNP_{CB}$ synthesis (red).

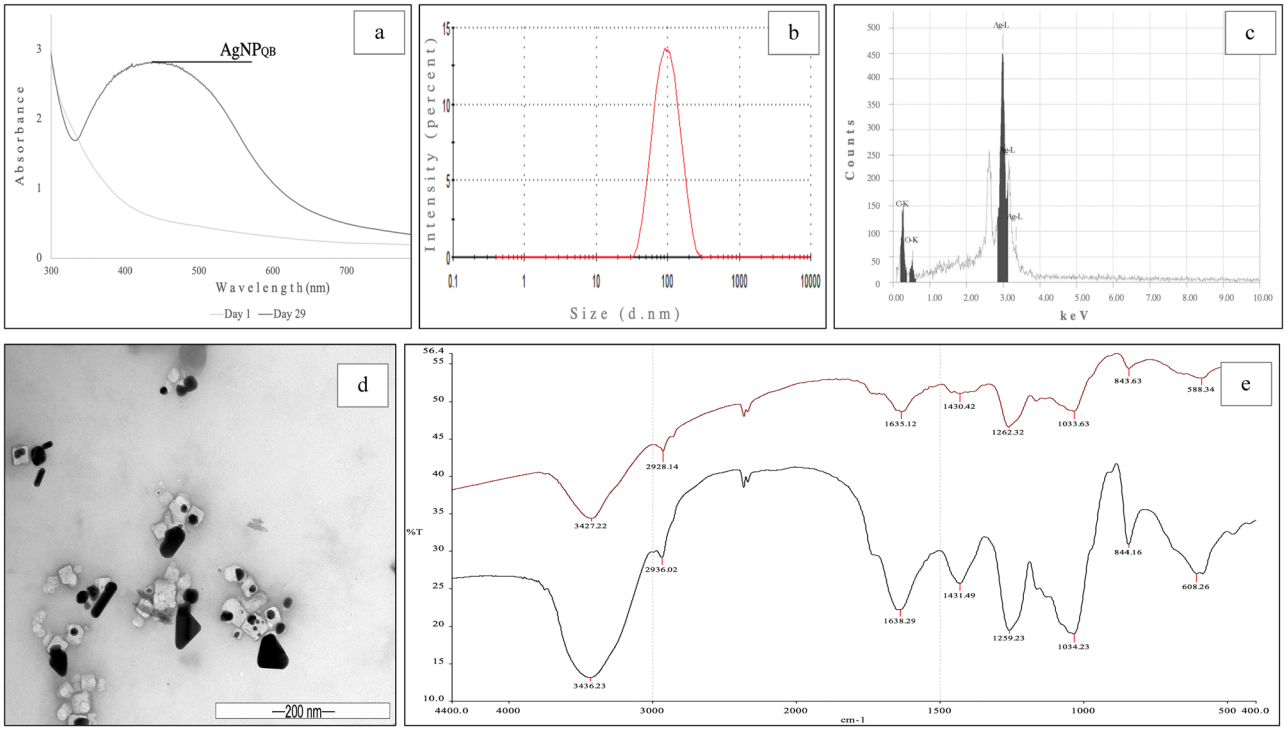

Figure 3: Characterization of biosynthesized $AgNP_{QB}$ using: (a) UV-vis spectroscopy, (b) DLS, (c) EDS of $AgNP_{QB}$ presenting 70% of Ag, (d) TEM imaging, and (e) FTIR of *H. clathratus* raw powder aqueous solution before (black) and after $AgNP_{QB}$ synthesis (red).

Table 2: Antibacterial activity of biologically synthesized $AgNP_{CB}$ and $AgNP_{QB}$

Bacteria	Inhibition zone (mm)	
	$AgNP_{CB}$	$AgNP_{QB}$
MDR *Acinetobacter baumannii* (MRSTAB) ATCC® BAA1790	17.2 ± 1.3	10.0 ± 1.0
ESBLs producing *Enterobacter cloacae* ATCC® BAA 2468	09.3 ± 0.6	ND
ESBLs producing *Escherichia coli**	ND	10.3 ± 0.6
Klebsiella pneumoniae carbapenemase (KPC) ATCC® BAA 2078	07.3 ± 5.7	00.0 ± 0.0
Methicillin-resistant *S. aureus* (MRSA) ATCC 43300	17.0 ± 0.0	10.3 ± 0.6
MDR *Pseudomonas aeruginosa* (MRSTPA) ATCC® BAA 2109	11.8 ± 0.3	08.8 ± 0.8
Vancomycin-resistant *Enterococcus faecium* (VRE) ATCC 700221	08.3 ± 0.6	00.0 ± 0.0
A. baumannii ATCC 19606	16.7 ± 2.5	14.3 ± 0.3
Salmonella Typhimurium ATCC 14028	13.0 ± 0.9	11.8 ± 0.8
E. coli ATCC 35218	12.0 ± 0.5	12.2 ± 0.3
K. pneumoniae ATCC® BAA 1706	11.3 ± 0.6	09.5 ± 0.5
Enterobacter cloacae ATCC 13047	8.0 ± 0.0	11.3 ± 0.6
P. aeruginosa ATCC 27853	13.0 ± 0.0	13.8 ± 1.4
Enterococcus faecalis ATCC 29212	00.0 ± 0.0	00.0 ± 0.0
S. aureus ATCC 25923	16.3 ± 0.6	15.3 ± 0.6
Proteus vulgaris ATCC 49132	9.3 ± 0.6	05.3 ± 4.6
Streptococcus pneumoniae ATCC 6305	11.3 ± 0.6	ND
*S. pneumoniae**	ND	00.0 ± 0.0

The diameter of the well (6 mm) was calculated within the zone of inhibition. The results shown are recorded as means ± standard deviation (SD). * – patient isolate. ND – no data.

produced $AgNP_{CB}$ were spherical and polygonal and ranged in size from 7 to 31 nm (Figure 2d). On the contrary, $AgNP_{QB}$ showed a variation in shapes, including spherical, triangle, quadrangular, and rod shapes, and their sizes ranged from 11 to 49 nm (Figure 3d).

3.2.4 EDS

EDS was used to conduct chemical composition analysis using a scanning electron microscope and to further confirm the presence of elemental Ag for verifying the reduction reaction. The analysis of synthesized AgNPs within *H. clathratus* showed the presence of elemental silver at 2.983 keV (Figures 2 and 3c).

3.2.5 FTIR

FTIR of $AgNP_{CB}$ unveiled a strongly stretched band at a lower frequency (3400.38 cm^{-1}) than the extract before $AgNP_{CB}$ formation (3413.56 cm^{-1}). Sharp bands were apparent at 2924.12 and 2854.96 cm^{-1}, all of which reduced in intensity after $AgNP_{CB}$ formation. A band at 1714.17 cm^{-1} shifted to a higher frequency (1,725 cm^{-1}) and reduced in intensity. The peaks from 1419.49 to 1646.16 cm^{-1} might be assigned to the involvement of C=C groups. A band disappeared at 1245.86 cm^{-1} after $AgNP_{CB}$ production, and a new band emerged in a lower frequency at 1023.61 cm^{-1} with a higher intensity; this may be a result of Ag bonding with O_2 in the C–O group (Figure 2e).

In contrast, $AgNP_{QB}$ showed strongly stretched bands at 3427.22 cm^{-1}, suggesting the hydroxyl group's involvement in the biosynthesis. The peak at 2928.14 cm^{-1} is attributed to the presence of aliphatic hydrocarbons. The reduction in the band 1635.12 cm^{-1} may indicate the involvement of benzene in the reduction of AgNPs. A bending of the peak at 1430.42 cm^{-1} was also observed with a lower intensity. Furthermore, medium stretching of bands was noted between 1262.32 and 1033.63 cm^{-1} with an evidence of lower intensity. The reduction in the intensity of the peak at 1033.63 cm^{-1} is attributed to the C–O group (Figure 3e).

3.3 Antibacterial activity of biologically synthesized AgNPs

3.3.1 Agar well-diffusion assay

To assess the biological activity of synthesized AgNPs, we performed an agar well-diffusion assay. Results are

shown in (Table 2) that presents the diverse responses of bacteria to AgNPs.

3.3.2 Microtiter MIC and MBC

The microtiter MIC and MBC assays showed various values depending on the tested bacteria with different responses to each of the biosynthesized AgNPs (Table 3). Some bacteria exhibited the same MIC and MBC values, indicating that the same concentration was both bacteriostatic and bactericidal.

3.3.3 Antibiofilm activity of AgNPs synthesized using *H. clathratus*

The CV staining assay of produced biofilm investigated the antibiofilm growth and development activity of AgNPs. As shown in (Table 4), all bacterial biofilms were resistant; however, MRSA was highly susceptible to $AgNP_{CB}$.

Table 4: Antibiofilm growth and development activity of $AgNP_{CB}$

Tested bacteria	Biofilm inhibition percentage (%)	
	AgNPs synthesized using *H. clathratus*	
	Conc. (100%)	Conc. (50%)
MDR *Acinetobacter baumannii*	1.0	1.5
MRSA	98.9	99.1
MDR *Pseudomonas aeruginosa*	4.3	4.6
Acinetobacter baumannii	2.4	3.0
Staphylococcus aureus	0	0.5
Pseudomonas aeruginosa	1.0	0.9

Conc. – concentration. All data were averaged before calculating the inhibition percentage.

4 Discussion

In the present study, phytochemicals from the alga *H. clathratus* were screened and used for the first time as a bioreductant to biosynthesize AgNPs. Producing inorganic AgNPs using "green" techniques is known to be eco-friendly, fast, and efficient. Other merits include their stability, endurance to high temperature, and low toxicity to humans, which can benefit medical applications [9].

The phytochemical screening using GC-MS identified saturated and unsaturated fatty acids, mostly, carboxylic acids, sugars, steroids, phytols, and other products. These components attributed to having an antibacterial activity or suggested as a reducing agent in the green synthesis of NPs [9]. Also, the detected fatty acids in algal extracts such as: palmitic, palmitoleic, stearic, oleic, and linoleic acids have a role in destroying the bacterial cell wall structure and function. They act as anionic surfactants, thus exhibiting their antibacterial and antioxidant activity [16].

Table 3: MIC and MBC of biologically synthesized $AgNP_{CB}$ and $AgNP_{QB}$

Bacteria	$AgNP_{CB}$ (mg/mL)		$AgNP_{QB}$ (mg/mL)	
	MIC	MBC	MIC	MBC
MDR *A. baumannii*	1.125 ± 0.0	1.50 ± 0.6	4.50 ± 0.0	4.50 ± 0.0
ESBLs producing *E. cloacae*	2.250 ± 0.0	6.00 ± 2.6	ND	ND
ESBLs producing *E. coli**	ND	ND	9.00 ± 0.0	9.00 ± 0.0
K. pneumoniae carbapenemase	4.500 ± 0.0	>18 ± 0.0	>18 ± 0.0	>18 ± 0.0
MRSA	2.250 ± 0.0	9.00 ± 7.8	9.00 ± 0.0	18.0 ± 0.0
MDR *P. aeruginosa*	0.938 ± 0.3	2.25 ± 0.0	4.50 ± 0.0	9.00 ± 0.0
A. baumannii	0.938 ± 0.3	1.500 ± 0.6	0.938 ± 0.32	1.125 ± 0.00
Salmonella Typhimurium	1.875 ± 0.6	2.250 ± 0.0	2.250 ± 0.00	4.500 ± 0.00
E. coli	0.938 ± 0.3	1.125 ± 0.0	1.125 ± 0.00	1.125 ± 0.00
K. pneumoniae	4.500 ± 0.0	9.000 ± 0.0	7.500 ± 2.60	>18 ± 0.0
E. cloacae	3.750 ± 1.3	4.500 ± 0.0	0.938 ± 0.32	1.688 ± 0.97
P. aeruginosa	0.938 ± 0.3	1.125 ± 0.0	3.750 ± 1.30	3.750 ± 1.30
Staphylococcus aureus	1.125 ± 0.0	2.250 ± 0.0	1.875 ± 0.65	3.750 ± 1.30
Proteus vulgaris	1.875 ± 0.6	ND	4.500 ± 0.00	4.500 ± 0.00

Results are shown as means ± SD. ND – no data.

The obtained AgNPs were characterized, and their biological activity was investigated against a variety of bacteria, including some MDR bacteria. We confirmed the formation of AgNPs, first using UV-vis spectroscopy showing peaks between 400 and 450 nm, specifically at 411 and 451 nm for $AgNP_{CB}$ and $AgNP_{QB}$, respectively. Thus, this signifies the surface plasmon resonance of silver, which is similar to [17] and other studies that used algae and plants as reducing agents [18,19].

DLS and TEM analyses were performed to evaluate the morphological properties and stability of AgNPs. $AgNP_{CB}$ and $AgNP_{QB}$ varied in size and shape (spherical, quadrangular, triangular, polygonal, and rods). Remarkably, biosynthesis using the algal powder produced smaller particles relative to those formed using the extract, albeit slowly. There was a noticeable inconsistency in the size of AgNPs in both DLS and TEM. To illustrate, DLS measures the hydrodynamic size of the particles involving its capping phytochemicals from the algal extract, while TEM measures the exact geometric size of NPs [20,21]. Despite these inconsistencies, our findings are mostly consistent with those of other researchers and are deemed acceptable, based on the assumption that the discrepancies are due to technical variability associated with the different equipment used rather than measurement errors.

EDS verified the presence of elemental silver in all nanosolutions. The optical absorbance at 3 keV is attributed to plasmon resonance of the metallic silver nanocrystals and is known as the Ag region [22]. This result is consistent with that of Shaik et al. [23], which used *Salvadora persica* L. root extract (Miswak) in the green synthesis of AgNPs.

FTIR was used to confirm the involvement of the algal functional groups in biomolecules during the reduction reaction [24]. The extracts were tested before and after the formation of AgNPs to compare the occurring shift in the resulting peaks. Use of metal salts to synthesize NPs requires a stabilizer against the van der Waals forces of attraction to avoid coagulation [25]. FTIR results accentuate the contribution of the hydroxyl group (O–H bond) at 3400.38 and 3427.22 cm^{-1} after $AgNP_{CB}$ and $AgNP_{QB}$ synthesis, respectively. The hydroxyl group particularly has been proven to reduce the metal ions of silver to its atom "*nano*" form and conduct stability for formed NPs, hence its ability to increase oxygen bonding. These findings are compatible with those observed in earlier studies [26,27].

Hydroclathrus clathratus has been used as an antitumor, antioxidant, and antibacterial agent [28–30]; yet, to the best of our knowledge, there are no published studies on the biosynthesis of NPs from this algal species. Algae are considered as effective bio-nanofactories for synthesizing metallic NPs; hence, they are abundantly available, and both dead and live biomass can be successfully used in the production of metallic NPs [31]. There are two acceptable antibacterial actions of AgNPs: contact killing by infiltrating bacterial cells and Ag^+ ion-mediated killing by generating reactive oxygen species (ROS) [32]. Oves et al. [33] used the fluorescent probe 2,7-dichlorofluorescein diacetate dyes to detect ROS production by AgNPs inside the bacterial cells. Results showed that free radicals' production in the media was associated with increased concentrations of AgNPs and incubation time. Many studies have demonstrated that bio-AgNP activity is concentration-dependent. More recent evidence proposes that bacterial aggregation and physiology are essential determinants that define the predominance of one or several of the proposed mechanisms for the AgNPs' antibacterial activity [34]. Moreover, studies have demonstrated that the relatively large surface area of smaller AgNPs facilitates the release of more silver ions, which penetrate the bacterial cell membrane leading to its death [35,36].

The *in vitro* biological tests against bacteria exhibited varied responses to the AgNPs, which were expressed by the diameter of the inhibition zone. AgNPs synthesized by algal methanol extracts were more effective, compared to the raw powder aqueous solution against bacteria. Remarkably, *A. baumannii* and *S. aureus*, both the sensitive and resistant strains, were the most affected by the algal methanol extracts, compared to other bacteria. Alavi et al. [37] studied the antibacterial activities of Ag, Cu, TiO_2, ZnO, and Fe_3O_4 NPs biologically synthesized using *Protoparmeliopsis muralis* lichen aqueous extract against MRSA, *E. coli*, and *P. aeruginosa*. The highest antibacterial activity was noticed with 0.1 M concentration of AgNPs against *P. aeruginosa*, MRSA, and *E. coli*, respectively. In contrast, $AgNP_{QB}$ was more effective against nonresistant *S. aureus*, *A. baumannii*, and *P. aeruginosa*. Studies have shown that Gram-positive bacteria are more susceptible to AgNPs, compared to Gram-negative bacteria due to their structural differences. Contradicting earlier findings [38,39], we found no biased antibacterial action against either Gram-positive or Gram-negative bacteria, which could be attributed to the charge difference between the AgNPs and bacterial cells [32].

Previous research work revealed the difficulty in biofilm growth and development inhibition, compared to cell attachment inhibition [15]. In this study, biofilm growth and development inhibition assay were used to evaluate the antibiofilm activity of AgNPs. We tested the antibiofilm

activity of $AgNP_{CB}$ against selected biofilm-forming bacteria in two concentrations. There were no notable differences between tested concentrations, and they profoundly inhibited the biofilm of MRSA with 99% inhibition. A study investigated the antibiofilm effect of bio-AgNPs fabricated using the *Artemisia scoparia* plant as a bioreductant and compared it to that of commercial AgNPs against 50 strains of *S. aureus*. They assessed this effect on bacterial biofilm at a molecular level, specifically on *icaABCD* genes, which are essential for biofilm formation. The results registered a more notable reduction and induction in *icaA* and *icaR* gene expression with the sub-MIC doses of biosynthetic AgNP contrasted to commercial AgNP [40]. Rolim et al. [41] synthesized AgNPs using the fungus *Stereum hirsutum* and two plant extracts (green tea and dill) and studied their antibiofilm activity against several bacterial strains of medical interest. MDR *P. aeruginosa* was highly susceptible to the AgNPs synthesized using *S. hirsutum* with 97% inhibition. Our findings, while dissatisfactory, further implicate the cost of bacterial antibiotics' resistance in its fitness and virulence in MRSA specifically.

A study suggested using nanotechnology to coat surgical devices and medical implants to control biofilm formation because NPs are capable of breaching the extracellular polymeric substance layer and the bacterial membrane of both Gram-positive and Gram-negative bacteria [42]. Even though we did not find this association with all tested bacteria, there are still controversies on whether the antibiotics' resistance to bacteria contributes positively or negatively to biofilm formation [43]. We recommend testing the effect of $AgNP_{CB}$ against MDR bacteria and on different stages of biofilm formation to comprehend their antibiofilm activity fully in the future.

5 Conclusions

This study has explored the capacity of the brown alga *H. clathratus* to produce NPs extracellularly following a rapid and biological approach. Different techniques were used to characterize the produced AgNPs and obtain a thorough background for the future application of formed AgNPs. Our research work has further proven the activity of biosynthesized AgNPs as antibacterial and antibiofilm agents with room for improvement. We also introduced many questions in need of further investigation regarding the consequences of drug resistance on bacterial fitness and bacterial biofilm formation, which may help in developing antibacterial/antibiofilm drugs and improving the fields of biotechnology and health altogether.

Acknowledgments: The authors would like to thank the Deanship of Scientific Research in King Saud University for funding and supporting this research work through the initiative of DSR Graduate Students Research Support (GSR). The authors would also like to acknowledge the help and advice provided by Prof. Nawal M. Almusayeib and Prof. Musarat Amina, from King Saud University, and Prof. Manal Awad, from King Abdullah Institute for Nanotechnology. Also, the authors thank Dr. Aref Elmubarak from the Plant Protection Department at King Saud University for performing the phytochemical screening of the algal samples.

Author contributions: M. M. A. and N. M. A. prepared the research design and supervision; R. R. A. performed experiments and wrote the manuscript.

References

[1] Baptista PV, McCusker MP, Carvalho A, Ferreira DA, Mohan NM, Daniela AF, et al. Nano-strategies to fight multidrug resistant bacteria—"a battle of the titans". Front Microbiol. 2018;9:1441.

[2] Al-Hajoj S, Varghese B, Shoukri MM, Al-Omari R, Al-Herbwai M, AlRabiah F, et al. Epidemiology of antituberculosis drug resistance in Saudi Arabia: findings of the First National Survey. Antimicrob Agents Chemother. 2013;57(5):2161–66.

[3] Zowawi HM, Balkhy HH, Walsh TR, Paterson DL. β-Lactamase production in key Gram-negative pathogen isolates from the Arabian Peninsula. Clin Microbiol Rev. 2013;26(3):361–80.

[4] Hoiby N, Bjarnsholt T, Givskov M, Molin S, Ciofu O. Antibiotic resistance of bacterial biofilms. Int J Antimicrob Agents. 2010;35(4):322–32.

[5] Shannon E, Abu-Ghannam N. Antibacterial derivatives of marine algae: an overview of pharmacological mechanisms and applications. Mar Drugs. 2016;14(4):81.

[6] Khan AR, Qari R. Antibacterial activities of brown seaweed *Sargassum boveanum* (J. Ag.) against diarrhea along the Coast of Karachi, Pakistan. J Environ Res Dev. 2012;6(3A):753–7.

[7] Torode TA, Marcus SE, Jam M, Tonon T, Blackburn RS, Herve C, et al. Monoclonal antibodies directed to fucoidan preparations from brown algae. PLoS One. 2015;10(2):e0118366.

[8] Pereira L. Seaweed flora of the European North Atlantic and Mediterranean. In: Kim SK, editor. Springer Handbook of Marine Biotechnology. Berlin: Springer Berlin Heidelberg; 2015.

[9] El-Sheekh MM, El-Kassas HY. Algal production of nano-silver and gold: Their antimicrobial and cytotoxic activities: a review. J Genet Eng Biotechnol. 2016;14(2):299–310.

[10] Davis TA, Volesky B, Mucci A. A review of the biochemistry of heavy metal biosorption by brown algae. Water Res. 2003;37(18):4311–30.

[11] Aleem AA. The marine algae of Alexandria. Alexandria: Egypt. Univ. Alexandria; 1993.

[12] Coppejans E, Leliaert F, Dargent O, Gunasekara R, De Clerck O. Sri Lankan Seaweeds – Methodologies and field guide to the dominant species. Brussels: Belgian Development Cooperation; 2009.
[13] Rajeshkumar S, Kannan C, Annadurai G. Green synthesis of silver nanoparticles using marine brown algae Turbinaria conoides and its antibacterial activity. Int J Pharm Bio Sci. 2012;3(4):502–10.
[14] Xie JL, Singh-Babak SD, Cowen LE. Minimum inhibitory concentration (MIC) assay for antifungal drugs. Bio Protoc. 2012;2(20):e252.
[15] Bazargani MM, Rohloff J. Antibiofilm activity of essential oils and plant extracts against *Staphylococcus aureus* and *Escherichia coli* biofilms. Food Control. 2016;61:156–64.
[16] Karimi E, Jaafar HZ, Ghasemzadeh A, Ebrahimi M. Fatty acid composition, antioxidant and antibacterial properties of the microwave aqueous extract of three varieties of *Labisia pumila* Benth. Biol Res. 2015;48(1):9.
[17] Rajoriya P. Green synthesis of silver nanoparticles, their characterization and antimicrobial potential [PhD thesis]. Sam Higginbottom University of Agriculture Technology and Sciences, India, 2017.
[18] Patra JK, Baek KH. Antibacterial activity and synergistic antibacterial potential of biosynthesized silver nanoparticles against foodborne pathogenic bacteria along with its anticandidal and antioxidant effects. Front Microbiol. 2017;8:167.
[19] Khalifa KS, Ragaa AH, Hanafy AH. Antitumor activity of silver nanoparticles biosynthesized by micro algae. J Chem Pharm Res. 2016;8(3):1–6.
[20] Tomaszewska E, Soliwoda K, Kadziola K, Tkacz-Szczesna B, Celichowski G, Cichomski M, et al. Detection limits of DLS and UV-Vis spectroscopy in characterization of polydisperse nanoparticles colloids. J Nanomater. 2013;2013:10.
[21] Chartarrayawadee W, Charoensin P, Saenma J, Rin T, Khamai P, Nasomjai P, et al. Green synthesis and stabilization of silver nanoparticles using *Lysimachia foenum*-graecum Hance extract and their antibacterial activity. Green Proc Synth. 2020;9(1):107–18.
[22] Fayaz AM, Balaji K, Girilal M, Yadav R, Kalaichelvan PT, Venketesan R. Biogenic synthesis of silver nanoparticles and their synergistic effect with antibiotics: a study against Gram-positive and Gram-negative bacteria. Nanomed Nanotechnol Biol Med. 2010;6(1):103–9.
[23] Shaik M, Albalawi GH, Khan ST, Khan M, Adil SF, Kuniyil M, et al. "Miswak" based green synthesis of silver nanoparticles: evaluation and comparison of their microbicidal activities with the chemical synthesis. Molecules. 2016;21(11):1478.
[24] Faghihzadeh F, Anaya NM, Schifman LA, Oyanedel-Craver V. Fourier transform infrared spectroscopy to assess molecular-level changes in microorganisms exposed to nanoparticles. Nanotechnol Environ Eng. 2016;1(1):1.
[25] Sivagnanam SP, Getachew AT, Choi JH, Park YB, Woo HC, Chun BS. Green synthesis of silver nanoparticles from deoiled brown algal extract via Box-Behnken based design and their antimicrobial and sensing properties. Green Proc Synth. 2017;6(2):147–60.
[26] Wang Z, Xu C, Zhao M, Zhao C. One-pot synthesis of narrowly distributed silver nanoparticles using phenolic-hydroxyl modified chitosan and their antimicrobial activity. RSC Adv. 2014;4(87):47021–30.
[27] Guerrini L, Alvarez-Puebla RA, Pazos-Perez N. Surface modifications of nanoparticles for stability in biological fluids. Materials. 2018;11(7):1154.
[28] Vimala T, Poonghuzhali T. *In vitro* antimicrobial activity of solvent extracts of marine brown alga, *Hydroclathrus clathratus* (*C. Agardh*) *M. Howe* from Gulf of Mannar. J Appl Pharm Sci. 2017;7(04):157–62.
[29] Kelman D, Posner EK, McDermid KJ, Tabandera NK, Wright PR, Wright AD. Antioxidant activity of Hawaiian marine algae. Mar Drugs. 2012;10(2):403–16.
[30] Wang H, Chiu LC, Ooi VE, Ang PO. A potent antitumor polysaccharide from the edible brown seaweed Hydroclathrus clathratus. Bot Mar. 2010;53(3):265–74.
[31] LewisOscar F, Vismaya S, Arunkumar M, Thajuddin N, Dhanasekaran D, Nithya C. Algal nanoparticles: synthesis and biotechnological potentials. Algae-organisms for imminent. Biotechnology. 2016;7:157–82.
[32] Yun'an Qing LC, Li R, Liu G, Zhang Y, Tang X, Wang J, et al. Potential antibacterial mechanism of silver nanoparticles and the optimization of orthopedic implants by advanced modification technologies. Int J Nanomed. 2018;13:3311.
[33] Oves M, Rauf MA, Hussain A, Qari HA, Khan AP, Muhammad P, et al. Antibacterial silver nanomaterial synthesis from *Mesoflavibacter zeaxanthinifaciens* and targeting biofilm formation. Front Pharmacol. 2019;10:801.
[34] Rodriguez-Serrano C, Guzman-Moreno J, Angeles-Chavez C, Rodriguez-Gonzalez V, Ortega-Sigala JJ, Ramirez-Santoyo RM, et al. Biosynthesis of silver nanoparticles by *Fusarium scirpi* and its potential as antimicrobial agent against uropathogenic *Escherichia coli* biofilms. PLoS One. 2020;15(3):e0230275.
[35] Chowdhury S, Basu A, Kundu S. Green synthesis of protein capped silver nanoparticles from phytopathogenic fungus *Macrophomina phaseolina* (Tassi) Goid with antimicrobial properties against multidrug-resistant bacteria. Nanoscale Res Lett. 2014;9(1):1–11.
[36] Raza MA, Kanwal Z, Rauf A, Sabri AN, Riaz S, Naseem S. Size- and shape-dependent antibacterial studies of silver nanoparticles synthesized by wet chemical routes. Nanomaterials. 2016;6(4):74.
[37] Alavi M, Karimi N, Valadbeigi T. Antibacterial, antibiofilm, antiquorum sensing, antimotility, and antioxidant activities of green fabricated Ag, Cu, TiO2, ZnO, and Fe3O4 NPs via protoparmeliopsis muralis lichen aqueous extract against multi-drug-resistant bacteria. ACS Biomater Sci Eng. 2019;5(9):4228–43.
[38] Chatterjee T, Chatterjee BK, Majumdar D, Chakrabarti P. Antibacterial effect of silver nanoparticles and the modeling of bacterial growth kinetics using a modified Gompertz model. BBA-Gen Subjects. 2015;1850(2):299–306.
[39] Al-Sharqi A, Apun K, Vincent M, Kanakaraju D, Bilung LM. Enhancement of the antibacterial efficiency of silver nanoparticles against Gram-positive and Gram-negative bacteria using blue laser light. Int J Photoenergy. 2019;2019:12.
[40] Moulavi P, Noorbazargan H, Dolatabadi A, Foroohimanjili F, Tavakoli Z, Mirzazadeh S, et al. Antibiofilm effect of green

engineered silver nanoparticles fabricated from *Artemisia scoporia* extract on the expression of icaA and icaR genes against multidrug-resistant *Staphylococcus aureus*. J Basic Microbiol. 2019;59(7):701–12.

[41] Rolim WR, Lamilla C, Pieretti JC, Díaz M, Tortella GR, Diez MC, et al. Comparison of antibacterial and antibiofilm activities of biologically synthesized silver nanoparticles against several bacterial strains of medical interest. Energy Ecol Environ. 2019;4(4):143–59.

[42] LewisOscar F, MubarakAli D, Nithya C, Priyanka R, Gopinath V, Alharbi NS, et al. One pot synthesis and anti-biofilm potential of copper nanoparticles (CuNPs) against clinical strains of Pseudomonas aeruginosa. Biofouling. 2015;31(4): 379–91.

[43] Cepas V, López Y, Munoz E, Rolo D, Ardanuy C, Martí S, et al. Relationship between biofilm formation and antimicrobial resistance in Gram-negative bacteria. Microb Drug Resist. 2019;25(1):72–9.

Appendix

Table A1: Phytochemicals identified in the MeOH extract and powder of *H. clathratus*

RT	Compound name Phytocomponents in the MeOH extract	Synonym
Saturated fatty acids		
24.135	*n*-Tridecanoic acid	Tridecanoic acid
25.885	Tetradecanoic acid	Myristic acid
27.115/29.185	Hexadecanoic acid	Palmitic acid
27.48	*n*-Pentadecanoic acid	NS
28.64/28.905	Palmitelaidic acid	9-Hexadecenoic acid
28.74	*cis*-9-Hexadecenoic acid	Palmitoleic acid
31.98	Octadecanoic acid	Stearic acid
34.68	Eicosanoic acid	Arachidic acid
Unsaturated fatty acids		
29.905	9-Octadecenoic acid	Elaidic acid
30.17	*cis*-10-Heptadecenoic acid	10*Z*-Heptadecenoic acid
31.555	9,12-Octadecadienoic acid (*Z*,*Z*)-	Linoleic acid
31.695	Oleic acid	Omega 9
33.78	Arachidonic acid	*cis*-5,8,11,14-Eicosatetraenoic acid
33.88	*cis*-5,8,11,14,17-Eicosapentaenoic acid	Eicosapentaenoic acid
34.17	9-Decenoic acid	Caproleic acid
Sugars		
27.055	Galactopyranose, 1,2,3,4,6-pentakis-*O*-(trimethylsilyl)-,.beta.-d-	Galactopyranose
27.655	1,5-Anhydro-D-sorbitol	Glucitol; (sugar alcohol)
33.54	Glyceryl-glycoside	NS
38.615	2-Monostearin	2-Stearoylglycerol
Carboxylic acids (derivatives)		
6.38	Formamide, *N*,*N*-diethyl-	Formamide
Steroids		
14.715	Glycerol	(Glycerin)
Others		
25.015	Borneol	(−)-Borneol (bicyclic monoterpenoids)
25.655/26.38	3,7,11,15-Tetramethyl-2-hexadecen-1-ol	Phytol
36.695	Hexadecanoic acid, 2,3-bis[(trimethylsilyl)oxy]propyl ester	NS
39.02	Octadecanoic acid, 2,3-bis[(trimethylsilyl)oxy]propyl ester	NS
RT	**Compound name** **Phytocomponents in the powder of H. clathratus**	**Synonym**
Saturated fatty acids		
27.47	*n*-Pentadecanoic acid	NS
27.71	Trimethylsilyl ether of glucitol	Glucitol; sorbitol (sugar alcohol)
29.05	Hexadecanoic acid	Palmitic acid
31.965	Octadecanoic acid	Stearic acid
34.67	Eicosanoic acid	Arachidonic acid
Unsaturated fatty acids		
28.625	*n*-Tridecanoic acid	Tridecanoic acid
28.725	*cis*-9-Hexadecenoic acid	Palmitoleic acid
28.885	Palmitelaidic acid	9-Hexadecenoic acid
30.16	*cis*-10-Heptadecenoic acid	10*Z*-Heptadecenoic acid
31.54	9,12-Octadecadienoic acid (*Z*,*Z*)-	Linoleic acid
31.61/31.705	Oleic acid	Omega 9
33.765	Arachidonic acid	*cis*-5,8,11,14-Eicosatetraenoic acid
33.87	*cis*-5,8,11,14,17-Eicosapentaenoic acid	Eicosapentaenoic acid
35.4	Oleanitrile acid; oleic acid with ammonia	NS

Table A1: Continued

RT	Compound name Phytocomponents in the powder of H. clathratus	Synonym
Sugars		
38.605	2-Monostearin	2-Stearoylglycerol
39.38	*N*-Acetyl-D-glucosamine, tetrakis(trimethylsilyl) ether, benzyloxime (isomer 1)	NS
Carboxylic acid		
39.525	Tetracosanoic acid	Lignoceric acid
Steroids		
45.855	24-Nor-22,23-methylenecholest-5-en-3.beta.-ol	(Sterol)
Others		
7.125	2,3,3-Trimethyl-, 1-butene	Alkene
25.645/26.37	3,7,11,15-Tetramethyl-2-hexadecen-1-ol	Phytol
36.69	Hexadecanoic acid, 2,3-bis[(trimethylsilyl)oxy]propyl ester	NS
38.705	Eicosanoic acid, 2,3-bis[(trimethylsilyl)oxy]propyl ester	NS

RT – retention time. NS – no synonyms. Synonyms were obtained via NIST, PubChem, ChEBI, and HMDB.